

ULTRA-LIGHT CONCENTRATORS FOR SOLAR THERMAL PROPULSION

Hironori Sahara

Japan Society for the Promotion of Science (JSPS)
7-44-1, Jindaiji-Higashi-Machi, Chofu, Tokyo 182-8522, JAPAN
(E-mail : sahamail@nal.go.jp)

Shinsuke Ezaki, Yasuhiro Matsui, Yoshihiro Nakamura

Hosei University

Morio Shimizu

National Aerospace Laboratory of Japan (NAL)

Abstract

This paper presents ultra-light electromagnetic wave concentrators (EMCs) developed in the National Aerospace Laboratory of Japan (NAL), especially the electromagnetic wave concentrator with variable focal length (EMC/VFL), and their representative applications to a solar ray concentrator for solar thermal propulsion (STP) and solar power station (SPS). The EMCs with 220 mm, 430 mm, and 640 mm in diameters were made of ultra-light aluminized or silvered polymer membrane. The EMC/VFL consists of a pair of rectangular reflectors of ultra-light thin materials such as reflective polymer membrane, each of which has a line focus due to appropriate bending moment and axial force. The variable bending moment and axial force make the reflector a highly precise paraboloidal concentrator with variable focal length, and its characteristics as a concentrator are calculated. The two focus lines intersect each other perpendicularly so that a point focus can be formed at the intersection. Unlike a conventional paraboloidal concentrator including an inflatable type, the EMC/VFL can be folded up very compactly, and oblong huge area for an electromagnetic wave receiver will be available in space. Because of their ultra-light weight and/or variable focal length, they can be more advantageous than the conventional or the inflatable type concentrator. In particular, the EMC/VFL is very promising when the concentrator area is quite large as for SPS, or over 10m² as for STP.

1. Introduction

Space missions which demand large amount of energy are often proposed. In the proposals, solar ray is usually regarded as an energy source, because the sun and its supplying energy are almost infinite, free, and continuous. In order to make the solar energy highly available, an instrument with appropriately wide area for solar ray concentration is necessary. The instrument is a paraboloidal concentrator in usual. The paraboloid is generated by rotation of a parabolic arc about the parabola's axis, and using a press mold makes highly precise paraboloidal concentrators be inexpensive and uncomplex in manufacture. They are seen in our everyday life or scientific research as home antennas for satellite broadcasting, antennas for space communications, and solar furnaces. As far as the concentration area is small, the paraboloidal concentrator made of reflective polymer membrane is one of the most promising items. However, it is very difficult to realize the paraboloidal antenna with widely huge area in space because of problems about its compactness, and cost for launch and deployment. Accordingly, inflatable type paraboloidal concentrators made of thermosetting reflective polymer membrane are often proposed in the world [1-4]. The inflatable paraboloid is enfolded by gas expansion after launch, and hardened in space by ultraviolet ray and so on. But no one can fold up paraboloid of revolution without causing any wrinkles which make its surface quite lower concentration efficiency. In addition, it has a sheet of canopy membrane, which lowers the concentration efficiency down to 60-80 percent [1-2]. Besides, a segmented rectangular concentrator was proposed [3]. The concentrator is comprised of 12 rigid rectangular reflectors. Although it can be folded comparatively compactly in a launcher, its storing efficiency is not necessarily available in arbitrary area. In the near future, the area of concentrators would be getting wider and wider to satisfy high efficiency and increasing demanded energy. Therefore, we propose a new concentrator, ultra-light EMC and EMC/VFL which consists of a pair of wide rectangular reflectors.

2. Ultra-light EMCs

2.1. Original EMCs

One of the STP studies in NAL has focused on the ultra-light EMC for high efficiency solar concentration. We made it possible by means of vacuum forming with aluminized or silvered polymer membrane of 25-127 micron in thickness and paraboloidal glass molds, as shown in Figs. 1 and 2. We obtained the EMCs of 220 mm, 430 mm, and 640 mm in diameters shown in Fig. 2. The EMC areal density is only 70 g/m^2 in using 50-micron polyester membrane, which makes concentrator weight be a hundredth of the conventional one. However, forming error less than several percents compared with the mold occurred, as shown in Fig. 3. Because of the error, concentrated solar image diameter of the EMC is 4-5 times larger than theoretical one, and 2 times larger than the mold one. In fact, the cross sectional shape of the EMC is surely expressed as a biquadratic equation. Figures 4 show how the measured EMC cross sectional shape concentrates solar rays, and the solar image at the focus has keen peak and broad foot. The answer to obtain a highly precise paraboloidal EMC is that the forming is conducted with a new mold which has a biquadratic expression surface with compensating the forming error. The new mold is now in manufacturing in NAL, and it will provide highly precise paraboloidal EMCs.



Fig. 1 Mold (left) and Ultra-light EMC (right)



Fig. 2 EMCs of 220 mm, 430 mm, and 640 mm in diameter

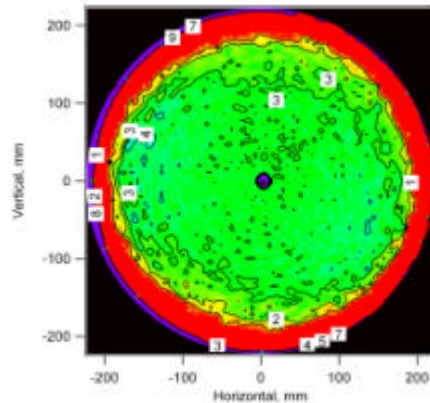
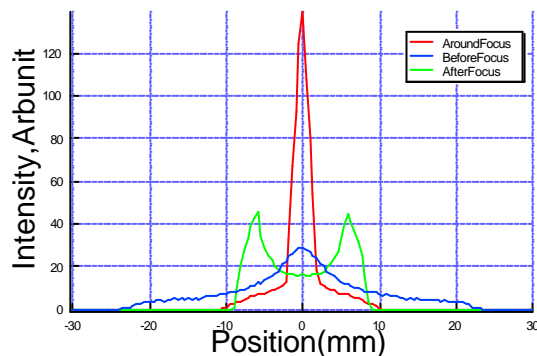
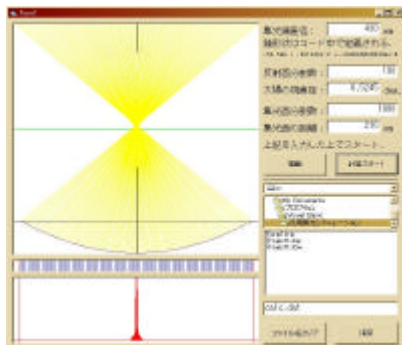


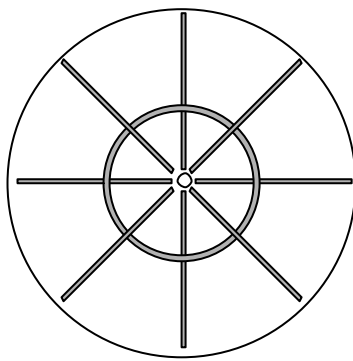
Fig. 3 Forming error in percentages compared with the mold



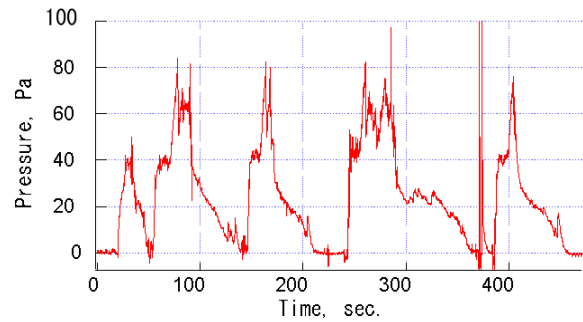
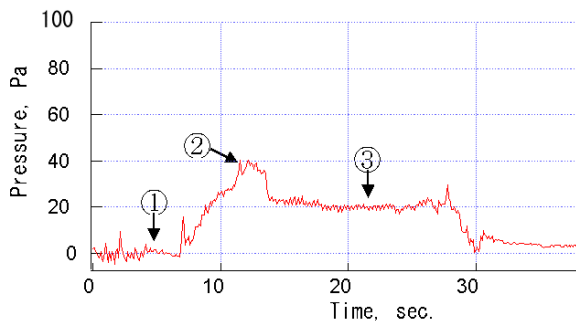
Figs. 4 Concentration simulation result of EMC with a biquadratic expression

2.2. KUMONOSU EMCs

The original EMC has only a circular groove for reinforcement, which is formed by sealing material for vacuum sealing, around its reflective and concentrating surface. The groove serving as maintaining the 3-dimensional surface shape, results in increasing the buckling strength and durability against external force to some extent. Even if the surface is transformed and buckled by external force, it recovers the original shape while the transformation is small. However, once the transformation exceeds a limit, it never recovers. Arranging the concentric and/or radial grooves for reinforcement mitigates the weakness. The grooves are arranged like cobweb (*KUMONOSU* in Japanese) on the reflective surface of the EMC as shown in Figs. 5, and the *KUMONOSU* EMC has the *KUMONOSU* grooves on its reflective surface (in patent pending, 2002-239694, Japan). The *KUMONOSU* grooves raise buckling strength and durability of the EMC, as shown in Figs. 6. In addition, the *KUMONOSU* grooves recover the EMC reflective surface buckling to the original shape even if the relatively large transformation occurs. Optimization to determine the most suited patterns of the *KUMONOSU* grooves on the *KUMONOSU* EMCs is now in progress.



Figs. 5 A *KUMONOSU* pattern (left), and *KUMONOSU* EMC (right)



Figs. 6 Buckling strength against pressure of the original (left) and the *KUMONOSU* EMC (right)

3. EMC/VFL

The EMC/VFL (in patent pending, 2001-320563, Japan) consists of a pair of rectangular reflectors of ultra-light thin materials such as reflective polymer membrane which has 25-127 micrometer in thickness. Its reflective surface is aluminized or silvered on a sheet of acryl, polyester, or polyimide. By avoiding using paraboloid of revolution, the concentrator will settle the issues about its weight, compactness, and cost for launch and deployment. That is, the EMC/VFL is rolled up very compactly in launch and enfolded smoothly in space without causing any wrinkles which quite lower concentration efficiency of the reflectors. Each of the reflectors has a line focus, because it is formed into a parabola sheet as shown in Fig. 7. Concentrations along horizontal and vertical directions are charged to the first and second reflectors, respectively. The two focus lines intersect each other perpendicularly so that a point focus can be formed at the intersection. By changing either or both of the focal lengths, the shape of focal image or the concentration ratio is changed to meet a demand.

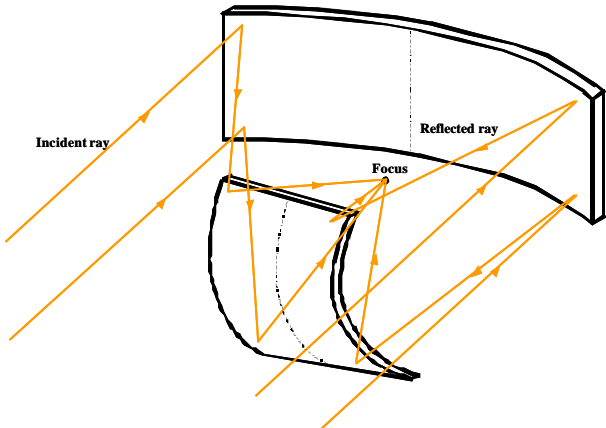


Fig. 7 Principle of EMC/VFL

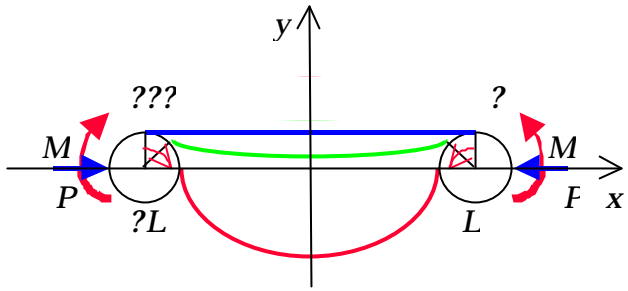


Fig. 8 Bending the reflector

In order to obtain a parabola and change its focal lengths, appropriate bending moment and axial force are imposed on the sheet of membrane as shown in Fig. 8. Imposing only bending moment on the sheet indeed makes it into a concentrator, but its shape becomes a circular arc which has not-so-good concentration characteristics. Appending axial force to the sheet bent by the bending moment makes it a highly precise parabola, since boundary conditions at its edges can be adjusted. Its characteristics as a concentrator are estimated by solving a given differential equation. The solution is expressed by complete elliptic integral of the first kind, and is approximately expressed as a quadratic function of Eq. 1 by Taylor expansion,

$$y \approx \frac{1}{4f}x^2 + Const., \quad (1)$$

where f represents the focal length and is expressed by a function of the bending moment and axial force, M, P , as shown in Fig. 9, or rotation angle of structure and interval between the structures, θ, L .

$$f \approx f(M, P) \approx f(\theta, L). \quad (2)$$

Before the fabrication of the EMC/VFL based on this concept, we realized an ultra-light EM wave concentrator with a fixed focal length (EMC/FFL) by applying sheets of very thin and ultra-light silvered polymer membrane to the pair of reflectors (in patent pending, 2001-147202, Japan). It successfully received EM wave from a Japanese broadcast satellite, as seen in Fig. 10.

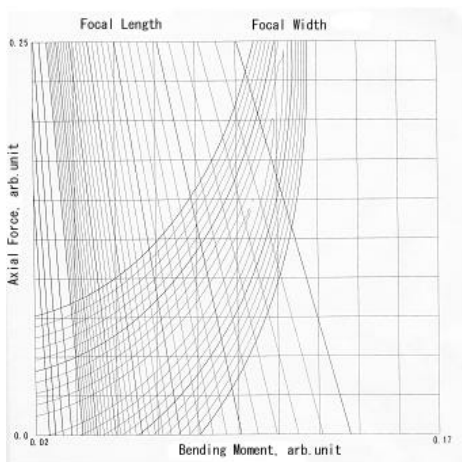


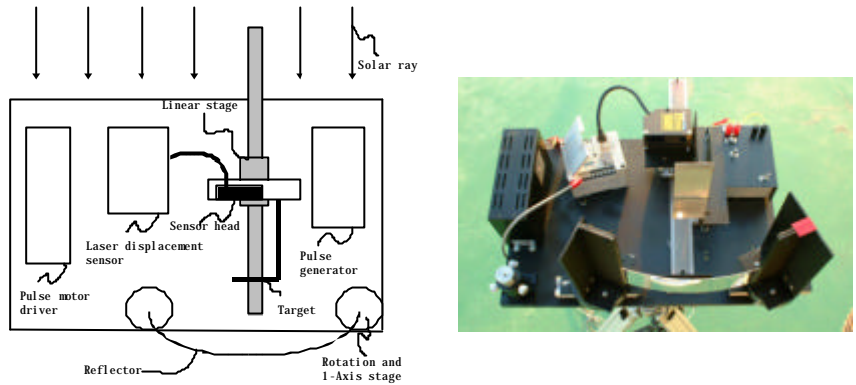
Fig. 9 Bending the reflector



Fig. 10 EMC/FFL in operation

In the following, we advanced the EMC/FFL to an EMC/VFL. We fabricated a test stand of the first

reflector in Figs. 11. A sheet of super-gloss aluminum (80 mm x 300 mm x 0.3 mm) was used as the reflector material instead of polymer membrane. A pair of rotation stages on uniaxial stages gives bending moment and axial force to the sheet. The reflected image is illuminated on a target, which is on a pulsed linear stage and distance between the target and reflector is changeable. A digital camera and a laser displacement sensor measure the focal image and length, respectively. The edges of reflector can be set free from the axial force.



Figs. 11 A test stand of the 1st reflector



Fig. 12 A concentrated line image

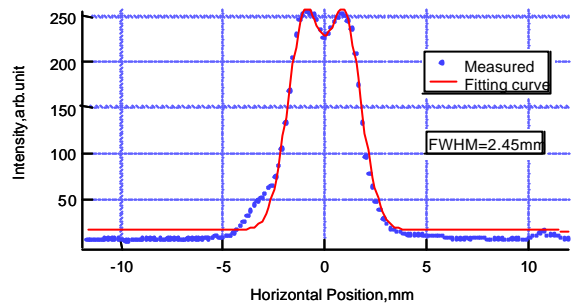


Fig. 13 Intensity distribution, in the case of axial-force-free

In the axial-force-free case, the concentrated image on the target was taken (Fig. 12) and the intensity distribution of the concentrated line image (Fig. 13) was acquired. A depression in the distribution was caused by a shadow of the target itself in front of the reflector. By supposing the distribution formed a Gaussian subtracting another Gaussian, curve fitting of the distribution including the depression was conducted. The width of the concentrated line image was defined as a function of full width at half maximum (FWHM) of the positive Gaussian. The dependence of the concentrated line width on the distance between the reflector and the target, was acquired in a given rotation angle as shown in Fig. 14. It was fitted by a quadratic function and the focal length was decided at the minimum width.

On the various rotation angles of the rotation stages, the widths of the distributions were acquired. The variable focal length worked very well in the axial-force-free case, as shown in Fig. 15. The focal length and width are 1.18 and 1.5 times larger than the theoretical ones, respectively.

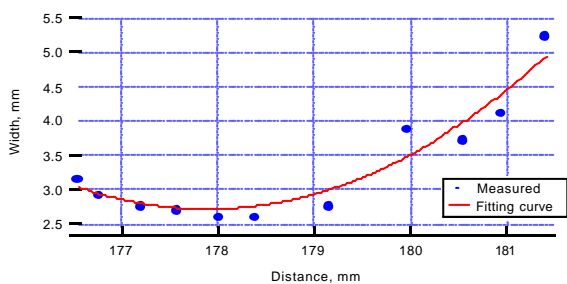


Fig. 14 Dependence of the width on the distance

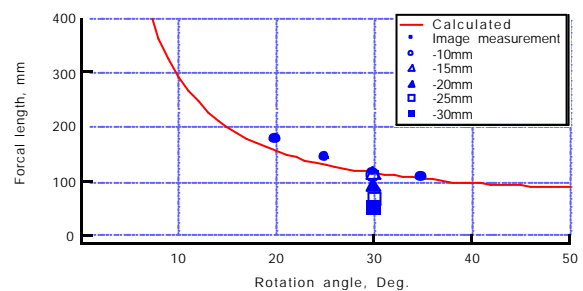


Fig. 15 Variable focal length

Next, the concentrated line widths were acquired in the case imposing axial force. The rotation angle was always fixed to be 30 degrees. The variable focal length was examined to work by the same way as in the axial-force-free case. The larger the axial force, the smaller the acquired focal length, as shown in Fig. 15. In Fig. 15, -10 mm, -15 mm, and so on mean the difference from initial interval between rotation axes of the rotation stages at the reflector edges. The focal width is nearly equal to the theoretical one when the interval between the support structures is about 10 mm smaller than the initial one. Figure 16 shows dependence of ratio of the focal width to the theoretical one on the interval. The width increases when the interval was too small or too large. There is an optimum of the axial force in imposing a bending moment. In this way, imposing axial force is good for a forming more precise parabola because the boundary condition at the edges is adjustable, and is more suitable for its functioning as a concentrator.

Thus, the variable focal length worked very successfully by applying appropriate bending moment and axial force imposed on the reflector.

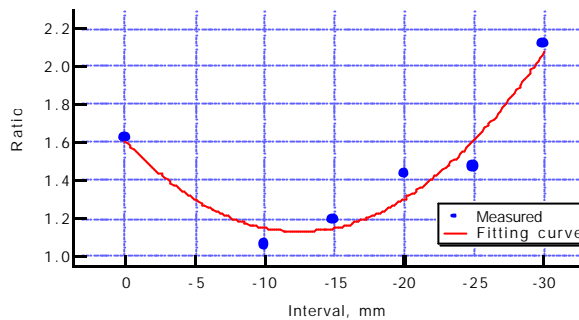
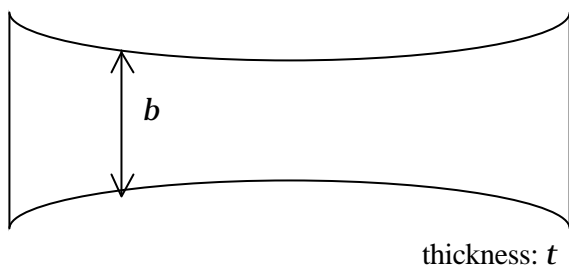


Fig. 16 Ratio of focal line width to theoretical one

4. Further advancing elements

4.1. Unrectangular reflector

The reflector is not necessary to be rectangular. If the most precise parabola is desired, moment of inertia of area is adjusted so that bending moment can form its deflection curve into an exact parabola. It is better for adjustment of the moment of inertia of area to adjust width of the reflector. The width is determined in Eq. (3), where M and E mean a given bending moment and Young's modulus, respectively. The shape of the reflector sheet forms as shown in Fig. 17. Using the sheet of this forms a very-highly precise parabola with variable focal length within a given range. If required focal length is predetermined, the sheet dimensions are decidable. The obtained parabola can be stricter than that of the rectangular reflector even in the case imposing axial force.



$$\frac{M}{Ebt^3/12} = \frac{d^2 y/dx^2}{\left(\frac{dy}{dx}\right)^{3/2}}, \quad y = \frac{1}{4f}x^2 \quad (3)$$

$$b = \frac{24Mf}{Et^3} \left(\frac{x}{2f}\right)^{3/2}$$

Fig. 17 Unrectangular reflector

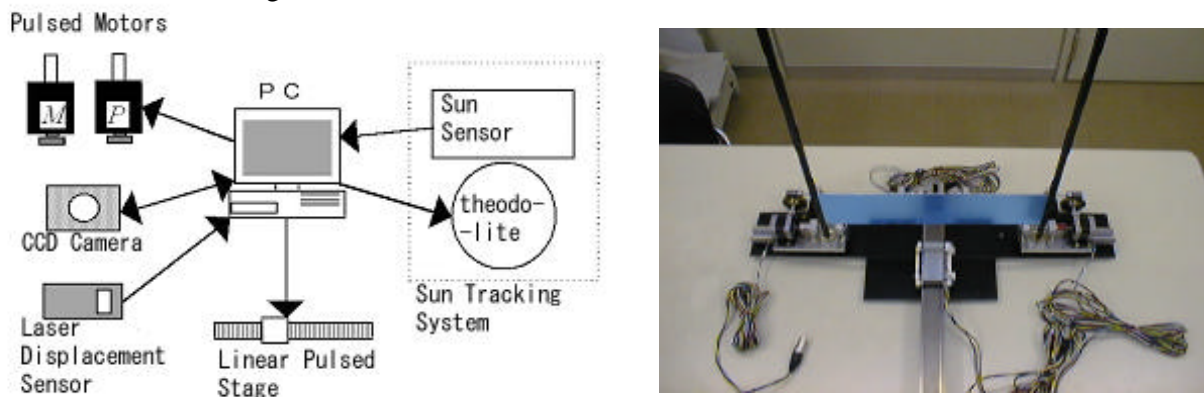
4.2. Driving system

We fabricated a driving system to impose the bending moment and axial force on the reflector sheet, which system consists of a pair of rotation parts on a uniaxis stages, as shown in Figs. 18. Each of the rotation parts has a driving system such as a pulsed motor or piezo actuator which rotates a worm gear with large gear ratio. The uniaxis stages are driven by another driving system to change the interval of a pair of the rotation

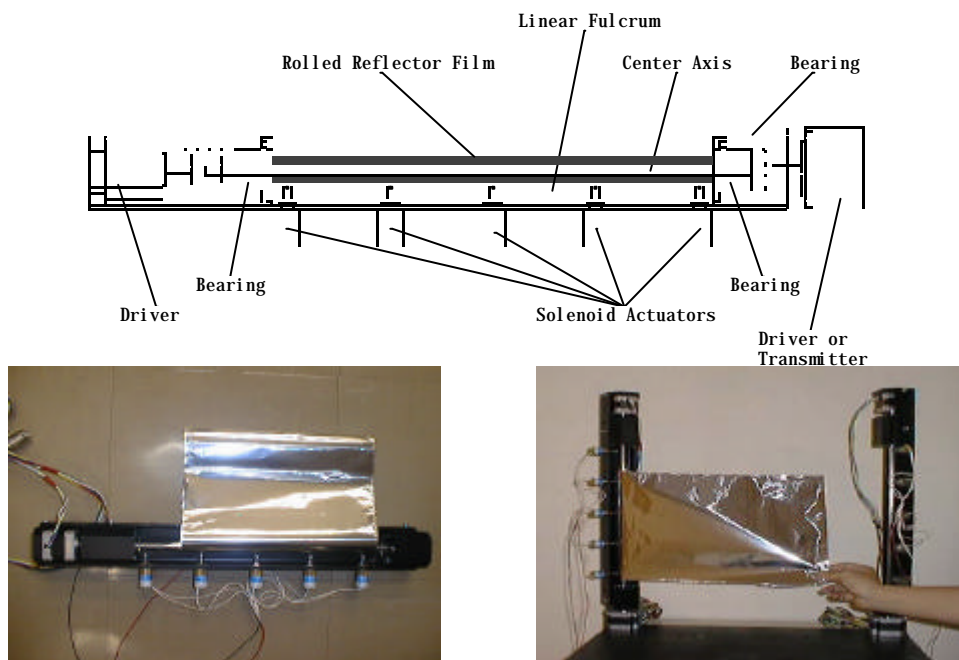
parts, which transmitted the symmetric motion with the stages simultaneously in the system. Thus, we are improving the EMC/VFL in order to realize precise positioning with good reproducibility.

4.3. Folding and exchanging mechanism

In space, it is not easy to exchange the reflector sheet even if its surface is polluted to decrease the reflectance by space radiation and/or atomic oxygen effects. Then, we are studying *folding and exchanging system* (FEM, in patent pending, 2002-302695, Japan) of thin film, shown in Figs. 19. The FEM has two coaxial axes of rotation, one of which supplies and rewinds the film, and the other imposes the bending moment on the exposed film sheet. The FEM is put on the driving system related above and applies the axial force to the exposed film sheet. A concentrator consists of a pair of the FEMs for supplying and rewinding the film. The FEM for supplying folds up the reflector sheet very compactly and the interval of a pair of the FEMs is a minimum until its operation. When needed, the FEM for rewinding pulls the film sheet from the one for supplying and the interval between them increases gradually. At the moment of a given interval between the both, the FEMs impose the bending moment on the reflector sheet, and necessary axial force is applied by adjusting the interval of the FEMs. If the reflector surface exposed in space is deteriorated, one of the FEMs rewinds the sheet in supplying the sheet by the other simultaneously. Thus, the EMC/VFL with keeping always-fresh surface with high reflectance will be realized.



Figs. 18 EMC/VFL with driving system



Figs. 19 Folding and exchanging mechanism

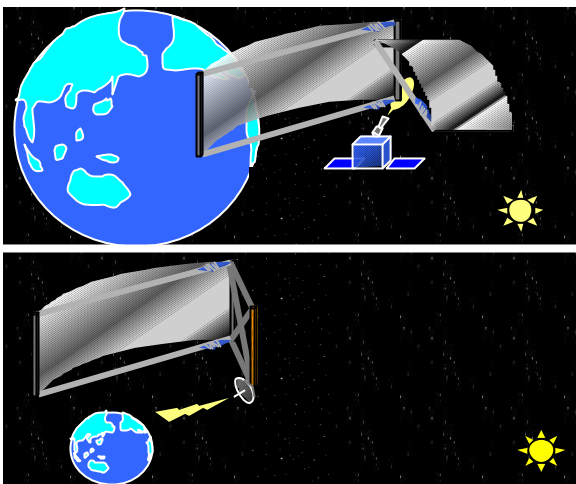
5. Applications

NAL has already started STP heating test with the ultra-light EMC made of aluminized polyester membrane, and is designing a STP system for orbit transfer of micro satellites. Figure 20 shows its pre-BBM model, which has a STP thruster and the EMC of 430mm in diameter.

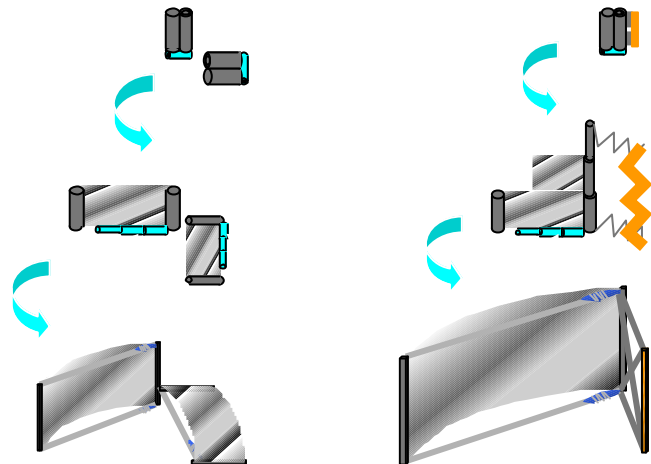
By applying the EMC/VFL to a solar concentrator of STP [5-16] or SPS [17] as shown in Figs. 21, it is advantageous because of its ultra-light weight and compactness. In general, typical STP and SPS demand 10 kW and 1 GW order of solar power. Here, assumption is as follows. A pair of reflectors are used in STP to obtain point focus on a STP thruster, and a reflector is used in SPS to obtain line focus on linear solar cell. This is for the reason why STP desires high concentration degree to achieve high propellant temperature while SPS demands low concentration degree in order not to lower the conversion efficiency and damage the solar cell thermally. For acquisition of the quantity of power, the concentrator of STP and SPS require 7.14 m^2 and $7.14 \times 10^5 \text{ m}^2$ of their solar ray receiver, respectively, from 1.4 kW/m^2 solar power density in space. In the case of the inflatable type concentrators including rim support structures ($0.775\text{-}0.94 \text{ kg/m}^2$ in areal density [2]), the concentrators weigh $5.54\text{-}6.72 \text{ kg}$ and $5.54\text{-}6.72 \times 10^5 \text{ kg}$, respectively. On the other hand, in the case of the EMC/VFL, weights of the concentrators including support structures are estimated at 7.0 kg and $2.23 \times 10^5 \text{ kg}$, respectively. This is for the reason why the weight of the inflatable type is proportional to its area and the weight of the EMC/VFL is proportional to length of its support structures. This means that there is surely a critical size and the EMC/VFL is more profitable than the inflatable type one when the area is large to some extent. First of all, the EMC/VFL is superior to the inflatable type with respect to not only mass but also compactness. The reflector can be rolled up very compactly because the material of it is very thin aluminized or silvered polymer membrane. Secondly, it is possible to be folded up without causing any wrinkles which quite lower concentration efficiency. The support structures are able to expand and contract. Therefore, the EMC/VFL can be contracted in the room of launcher and deployed in space for its operation. The way to impose bending moment and axial force to the reflector is considerable issue in the next phase. Besides, it is possible for the EMC/VFL to be used as a radio wave receiver. In this case, the surface of the reflector is not



Fig. 20 NAL pre-BBM model of STP with an ultra-light EMC.



Figs. 21 Applications for STP (upper) and SPS (lower)



Figs. 22 Folding up the concentrator compactly

necessary to be reflective, but may be a mesh of reflector. The mesh reflector should have little rigidity to be bent by imposing force. The rigidity would be given by top and bottom support structures of the reflector on the picture of the right in Fig. 22. This is one method to realize a widely-large-areal and very-light antenna by the EMC/VFL. This antenna will be used for the communication between deep space and the earth.

6. Summary

We presented the ultra-light EMC and EMC/VFL, and their uses for STP and SPS. Fabricating and testing the EMC/VFL confirmed its variable focal length capability and it worked very successfully. They can be more advantageous than the conventional or the inflatable type concentrator. In particular, the EMC/VFL is very promising when the concentrator area is quite large as for SPS, or over 10 m² as for STP.

Bibliography

- [1] P. E. Frye, J. A. McClanahan, "Solar Thermal Propulsion Transfer Stage for the First Pluto Mission," AIAA-93-2601, 29th Joint Propulsion Conference & Exhibit, Monterey, CA, June 28-30, 1993.
- [2] David Lichodziejewski, Dr. Costas Cassapakis, "Inflatable Power Antenna Technology," AIAA 99-1074, 1999.
- [3] G. Grossman, G. Williams, "Inflatable Concentrators for Solar Propulsion and Dynamic Space," Journal of Solar Energy Engineering, Vol. 112, pp.229-236, November 1990.
- [4] R. Partch, P. Frye, "Solar Orbit Transfer Vehicle Space Experiment Conceptual Design," AIAA-99-2476, 35th Joint Propulsion Conference & Exhibit, Los Angeles, California, June 20-24, 1999.
- [5] R. Joseph Cassady, "In-Space Propulsion Systems and Technologies," AIAA 99-2610, 35th Joint Propulsion Conference & Exhibit, Los Angeles, California, 20-24 June 1999.
- [6] Shoji, J. M., "Solar Rocket Component Study," AFRPL TR-84-057, AD-A154 186, 1985.
- [7] Kudija, C., "The Integrated Solar Upper Stage (ISUS) Engine Ground Demonstration (EGD)," AIAA Paper, AIAA-96-3043, 1996.
- [8] For example, Workshop Proceedings, NASA Solar Thermal Propulsion Workshop, MSFC, NASA, March 19-20, 1997.
- [9] Kennedy, C. F., Jacox, M., "The Integrated Solar Upper Stage (ISUS) Program," AIAA Paper, AIAA-95-3628, 1995.
- [10] Shimizu, M., et al., "Very Small Solar Thermal Thruster Made of Single Crystal Tungsten for Micro/Nanosatellites," 36th Joint Propulsion Conference & Exhibit, AIAA-2000-3832, Huntsville, Alabama, July 16-19, 2000.
- [11] Shimizu, M., et al., "Solar Thermal Thruster Made of Single Crystal Molybdenum," 47th IAF, Beijing, China, October 7-11, 1996, IAF-96-S.4.01, Acta Astronautica, Vol. 41, No. 1, pp. 23-28, 1997.
- [12] Shimizu, M., et al., "JSUS Solar Thermal Thruster and Its Integration with Thermionic Power," Proc. STAIF-98, pp. 364-369, 1998.
- [13] Shimizu, M., et al., "Single Crystal Mo Solar Thermal Thruster for Micro/nanosatellites," 49th IAF, IAF-98-S.6.01, Acta Astronautica, Vol. 44, No. 7, pp. 345-352, 1999.
- [14] Itoh, K., et al., "Solar Thermal Rocket as an Apogee Engine For Japanese launch Vehicles," ISTS-98-a-2-01, 21st International Symposium on Space Technology and Science, Omiya, Japan, May 24-31, 1998.
- [15] Sahara, H., et al., "Single and Opposed-Cavity Solar Thermal Thrusters Made of Single Crystal Tungsten," Proc. of 3rd International Conference on Spacecraft Propulsion, pp. 195-201, Cannes, France, October 10-13, 2000.
- [16] Sahara, H., et al., "Opposed-Cavity Solar Thermal Thruster Made of Single Crystal Tungsten," IEPC-01-214, 27th International Electric Propulsion Conference, Pasadena, California, October 15-19, 2001.
- [17] J. Martin, B. Donahue, M. Henley, J. McClanahan, "In-Space Transportation for GEO Space Solar Power Satellites," AIAA 2000-3857, 36th Joint Propulsion Conference, Huntsville, Alabama, 17-19 July 2000.